TOPICAL REVIEW — Fundamental physics research in lithium batteries

All-solid-state lithium batteries with inorganic solid electrolytes: Review of fundamental science*

Xiayin Yao(姚霞银), Bingxin Huang(黄冰心), Jingyun Yin(尹景云), Gang Peng(彭刚), Zhen Huang(黄祯), Chao Gao(高超), Deng Liu(刘登), and Xiaoxiong Xu(许晓雄)†

Ningbo Institute of Materials Technology and Engineering, Chinese Academy of Sciences, Ningbo 315201, *China*

(Received 14 May 2015; revised manuscript received 30 June 2015; published online 7 December 2015)

The scientific basis of all-solid-state lithium batteries with inorganic solid electrolytes is reviewed briefly, touching upon solid electrolytes, electrode materials, electrolyte/electrode interface phenomena, fabrication, and evaluation. The challenges and prospects are outlined as well.

Keywords: all-solid-state lithium batteries, inorganic solid electrolytes, interface phenomena, rechargeable lithium batteries

PACS: 88.80.ff, 82.45.Gj, 68.35.Fx, 82.47.Aa **DOI:** 10.1088/1674-1056/25/1/018802

1. Introduction

Chemical energy storage, including lead acid batteries, nickel system batteries, and lithium ion batteries (LiBs), is considered to be the most promising energy storage technology for industrialization.[1] Among these, LiBs have many advantages such as light weight, high energy density, high power density, and long life, and they are overwhelmingly preferred by designers for use in portable electronic devices such as cell phones and laptops.[1,2] However, overcharging or short-circuiting can lead to high temperature and result in fire or explosion due to the presence of flammable organic electrolytes.[1,3] Fires and explosions of LiBs have been reported throughout the world. The developments of electric vehicles (EVs) and large-scale energy storage devices for new kinds of power stations greatly expand the market for LiBs, meanwhile, stricter safety requirements apply to LiBs. Since large numbers of LiBs are packed together in EVs or power stations, fire or explosion in an LiB could be disastrous. Safety has become the main obstacle for the wide application of LiBs. To meet this issue, all-solid-state lithium batteries (ASSLiBs) have entered the field.

An ASSLiB is composed mainly of cathode, anode, and solid electrolyte, as developed during the latter half of the 20th century.[4,5] ASSLiBs have a simpler structure than the traditional LiBs, and the simplified structure with a solid electrolyte enables higher energy density.[6] Solid electrolytes not only conduct Li^+ ions but also serve as the separator, as shown in Fig. 1. In ASSLiBs, no organic liquid electrolyte, electrolyte salt, separator, or binder is required, which dramatically simplifies the assembly process.[7] The operational principle of ASSLiBs is no different from the traditional LiBs. In the charge process, lithium ions deintercalate from the cathode material and transport to the anode through the electrolyte, while electrons drift to the anode by the external circuit. Lithium ions combine with electrons to form more complete lithium atoms. The discharge process is just the reverse.[1,2]

At present, ASSLiBs fall into two categories according to the electrolyte:[8] polymer-based ASSLiBs with polymer solid electrolytes and ASSLiBs with inorganic solid electrolytes. The advantages of polymer-based ASSLiBs include greater safety, easy preparation, and flexible shape.[9] However, many problems remain to be solved, such as the instability of the electrolyte/electrode interface, the narrow temperature range of polymers, and the poor mechanical stability.[10,11] By contrast, inorganic solid electrolytes are non-flammable and highly stable mechanically.[7] The replacement of liquid electrolytes with inorganic solid electrolytes is considered to be the ultimate solution for the safety issues.[12] Also, inorganic ASSLiBs have a wide electrochemical window, which could be operated under high cut-off voltage.

The four fundamental problems in ASSLiBs, shown in Fig. 2, are:

- changes of volume and stress in materials during the charge–discharge process, which affect the cycle life and safety;
- ion and electron migration of electrode materials, which affects specific capacity, specific power, and cycle life;
- ion migration of electrolytes, affecting specific capacity, specific power, and cycle life;
- solid-electrolyte/electrode interface structure, affecting

*Project supported by the National High Technology Research and Development Program of China (Grant No. 2013AA050906), the National Natural Science Foundation of China (Grant Nos. 51172250 and 51202265), the Strategic Priority Research Program of the Chinese Academy of Sciences (Grant No. XDA09010201), and Zhejiang Province Key Science and Technology Innovation Team, China (Grant No. 2013PT16).

†Corresponding author. E-mail: xuxx@nimte.ac.cn

© 2016 Chinese Physical Society and IOP Publishing Ltd

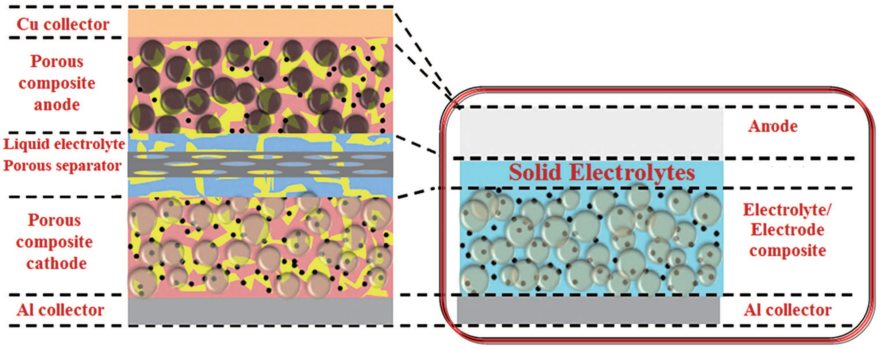


Fig. 1. Schematic illustration of traditional lithium ion battery and all-solid-state lithium battery.[1]

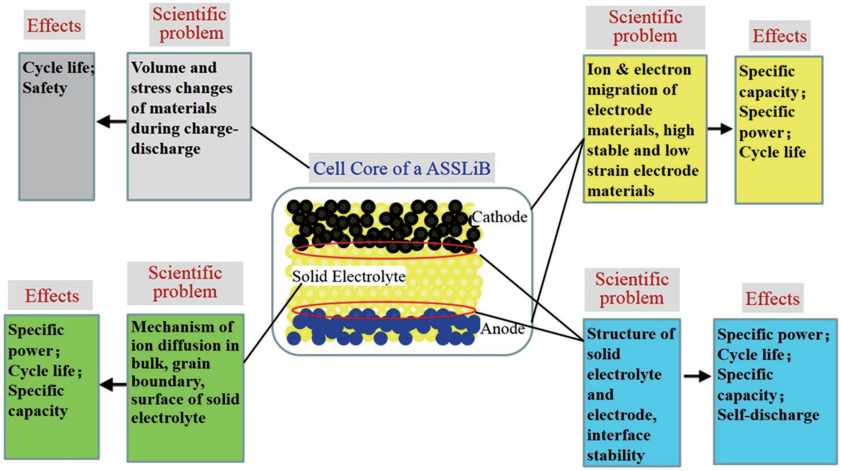


Fig. 2. The fundamental problems in ASSLiBs.

specific power, cycle life, specific capacity, and self-discharge.

The last two points are characteristic scientific problems of ASSLiBs and will be discussed in detail in this review.

2. Solid electrolytes

Solid electrolytes, also called superfast ionic conductors, are solid materials that exhibit a conductivity comparable with liquid electrolytes at working temperature, i.e., $> 10^{-2}$ S·cm^{-1}, and the activation energy is < 0.5 eV. Solid electrolytes conduct ions, and the charge carriers could be cations, anions, or ion defects; however, solid electrolytes' electron conductivity is negligible.

The temperature dependence of ion conductivity in solid electrolytes normally follows the Arrhenius law: $\sigma T = \sigma_{\rm o} \exp(E_{\rm a}/K_{\rm B}T)$, where T, $\sigma_{\rm o}$, $E_{\rm a}$, and $K_{\rm B}$ are the absolute temperature, an exponential factor, the activation energy of ion migration, and the Boltzmann constant, respectively. A linear relation should exist between $\lg \sigma T$ and $(1/T)$.

2.1. Oxide electrolytes

2.1.1. Perovskite type structure

Perovskite is a general term for a structural family of inorganic materials with the structure of $CaTiO_3$,[13] which has a general formula of ABO_3 with alkaline rare or earth metal ions in A sites and transition metal ions in B sites. The ideal perovskite has cubic symmetry with the space group $Pm3m$. The B cation and the A cation are 6-fold and 12-fold coordinated with the oxygen anions, respectively, as shown in Fig. 3.

A series of $Li_{3x}La_{2/3-x}TiO_3$ was synthesized with Li and La occupying the A positions. Inaguma *et al.* synthesized $Li_{3x}La_{2/3-x}TiO_3$, which exhibited a conductivity exceeding 10^{-3} S·cm^{-1} at room temperature (RT).[14] The abnormally high ion conductivity of perovskites has aroused strong interest among researchers. The structure of $Li_{3x}La_{2/3-x}TiO_3$ depends on the composition and the preparation conditions; tetragonal, cubic, or orthogonal structure could be obtained. The conductivity of perovskites is affected mainly by the atoms in the A position, since the size of the Li diffusion channel is determined by the A atoms. Furthermore, the occupation of high-valence La in A positions results in A vacancies, and Li ions transport by the vacancy mechanism. However, $Li_{3x}La_{2/3-x}TiO_3$ is not suitable for use as an electrolyte, since it is unstable when in contact with lithium metal. Lithium can quickly intercalate into the lattice of $Li_{3x}La_{2/3-x}TiO_3$ and reduce Ti^{4+} to Ti^{3+}.

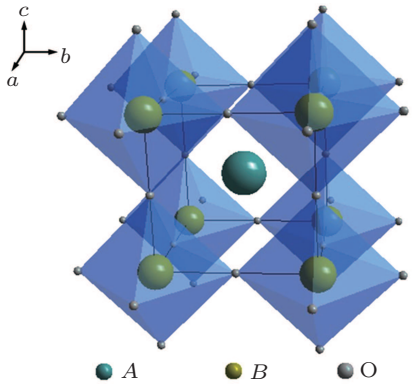


Fig. 3. Structure schematic of perovskite type electrolytes.

2.1.2. NASICON type structure

The compounds $NaM_2(PO_4)_3$ (M = Ge, Ti, Zr) were studied as early as the 1960s.[15] The structure was named NASICON (sodium (Na) super (S) ionic (I) conductor (CON)) in 1976, after the modifications $Na_{1+x}Zr_2Si_xP_{3-x}O_{12}$ ($0 \leq x \leq 3$), which exhibited high Na ion conductivity, were synthesized and characterized by Goodenough and Hong *et al.*[16] NASICON compounds have a general formula of $AM_2(BO_4)_3$, where the A site is occupied by alkali atoms (Li^+, Na^+, K^+), and the M site is occupied by tetra-valence ions (Ge^{4+}, Ti^{4+}, Zr^{4+}). The NASICON structure belongs to the $R\bar{3}c$ space group, and the skeleton structure consists of MO_6 octahedra and BO_4 tetrahedra. The BO_4 tetrahedra and MO_6 octahedra connect with each other by sharing corner O atoms, and form a three-dimensional rigid framework, which contains interconnected channels for A ion diffusion, as shown in Fig. 4. There are two kinds of positions for A ions, called AI (octahedral vacancies) and AII (tetrahedra vacancies). The A ions diffuse in the structure by jumping between AI and AII.

Lithium superfast ionic conductors are obtained with occupation of Li ions in A sites. Lithium ion conductivity in NASICON structure is related to the channel size, and high conductivity is obtained only when the channel size and the ion size match.[17] Subramanian *et al.* reported very low conductivity of $LiZr_2(PO_4)_3$, but it could be remarkably improved by substitution of (Hf, Zr, Ti, Sn).[18–20] The highest conductivity is exhibited by $LiTi_2(PO_4)_3$, indicating the importance of the match between diffusing ions and channel size.[17] The highest lithium ion conductivity was obtained for $LiTi_2(PO_4)_3$ with an optimum cell volume of 1310 Å^3. The $LiTi_2(PO_4)_3$ based system has been extensively investigated due to its high ion conductivity. The ion conductivity of $LiTi_2(PO_4)_3$ could be further enhanced with the substitution of M^{3+} for Ti^{4+}. Aono *et al.* studied the conductivity of the $Li_{1+x}Ti_{2-x}M_x(PO_4)_3$ (M = Al, Cr, Ga, Fe, Sc, In, Lu, Y, La) system, and the conductivity was increased more than one order of magnitude.[21] In particular, Al substitution was most effective, and a maximum conductivity of 7×10^{-4} S·cm^{-1} was obtained at 298 K for $Li_{1.3}Ti_{1.7}Al_{0.3}(PO_4)_3$.[21] Morimoto *et al.* prepared $Li_{1.3}Ti_{1.7}Al_{0.3}(PO_4)_3$ by mechanical milling, and its conductivity reached the order of 10^{-4} S·cm^{-1} at RT.[22] With the same preparation method, Xu *et al.* prepared a slightly different composition of $Li_{1.4}Al_{0.4}Ti_{1.6}(PO_4)_3$ with conductivity of 5.16×10^{-4} S·cm^{-1} at RT.[4] They also synthesized $Li_{1.4}Al_{0.4}Ti_{1.6}(PO_4)_3$ by spark plasma sintering; it possessed nano-grains with almost theoretical density,[4] and a very high conductivity of 1.12×10^{-3} S·cm^{-1} was obtained.[23]

The $Li_{1+x}Al_xGe_{2-x}(PO_4)_3$ (LAGP) system has been investigated due to its high electrochemical stability and wide electrochemical window.[25] At $x = 0.5$–0.6, it was reported to exhibit high conductivity and low activation energy at RT.[26] $Li_{1.5}Al_{0.5}Ge_{1.5}(PO_4)_3$ glass-ceramics were prepared to improve the conductivity,[27,28] and the high conductivity of 6.2×10^{-4} S·cm^{-1} was obtained. In recent years, some interesting results on the NASICON structure solid electrolytes have been obtained in our group at Ningbo Institute of Materials Technology and Engineering, Chinese Academy of Sciences.[24] At present, the third generation (G3) of $Li_{1.5}Al_{0.5}Ge_{1.5}(PO_4)_3$ based microcrystalline materials has been prepared at 100 kg scale, and the ion conductivity of G3 reaches 6.21×10^{-4} S·cm^{-1}. The relative density of G3 is over 97%. Figure 5(a) exhibits the ion conductivity of three generations (first, G1; second, G2; and third, G3). Values of the activation energy E_a, calculated by fitting the Arrhenius equation, are 0.39 eV, 0.36 eV, and 0.34 eV for G1, G2, and G3 $Li_{1.5}Al_{0.5}Ge_{1.5}(PO_4)_3$ at RT, respectively. Figures 5(b)–5(d) present SEM images of $Li_{1.5}Al_{0.5}Ge_{1.5}(PO_4)_3$ based microcrystalline materials. It can be seen that the grains of G3 are more uniform.

In summary, NASICON-structure fast ionic conductors exhibit high RT ion conductivity, high chemical stability, and a wide electrochemical window, and they are suitable for use as solid electrolytes in high voltage ASSLiBs. The future development will focus on optimization of the preparation process, enhancement of grain boundaries and grain conductivity, raising density to further improve RT ionic conductivity and expand the application fields.

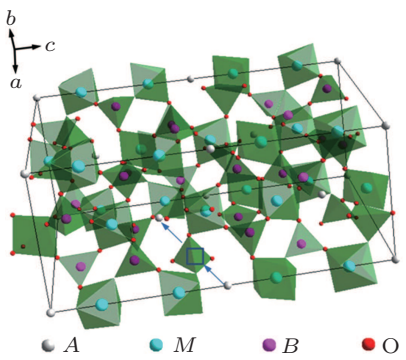


Fig. 4. Structure schematic of NASICON type electrolytes.

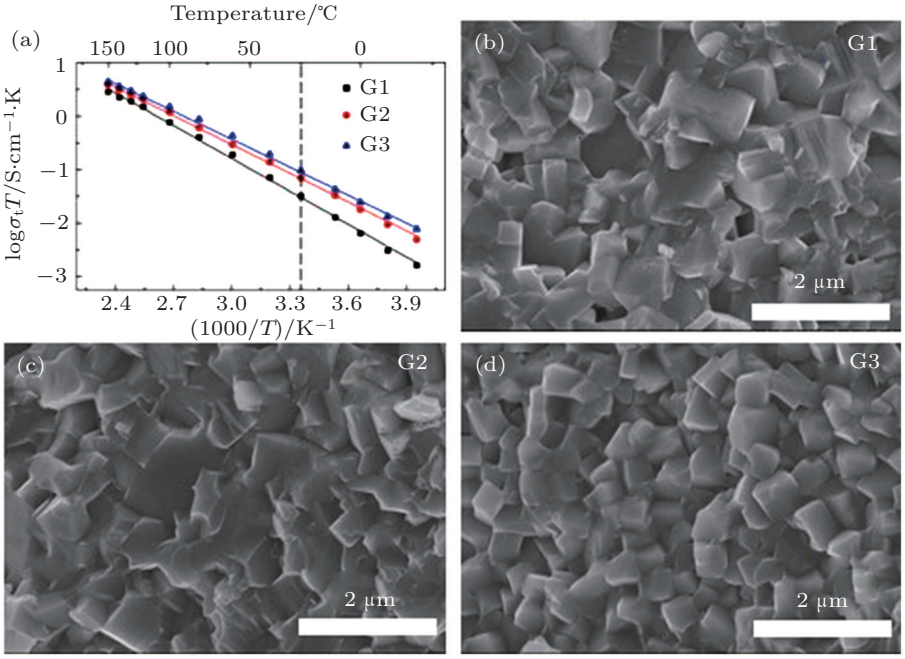


Fig. 5. (a) Temperature dependence of three generations' ionic conductivities and (b)–(d) SEM images of three generations of $Li_{1.5}Al_{0.5}Ge_{1.5}(PO_4)_3$-based microcrystalline samples.[24]

2.1.3. Garnet type structure

The garnet structure has a general formula of $A_3B_2Si_3O_{12}$ with space group *Ia*-3*d*, where *A* is an eight-coordination cation, and *B* is a six-coordination cation. The first Li-containing garnet structure $Li_3M_2Ln_3O_{12}$ (M = W, Te) was studied by Kasper *et al.* in 1969.[29] A new type of garnet structure, $Li_5La_3M_2O_{12}$ (M = Nb, Ta) was found by Mazza in 1988,[30] where Li occupies the 24d position in the tetrahedra and the 48g position in the octahedra,[31] as shown in Fig. 6. It exhibits high Li^+-ion conductivity and a wide electrochemical window.[32] $Li_5La_3M_2O_{12}$ (M = Nb, Ta) exhibits a conductivity of 10^{-6} S·cm^{-1} at RT, and the activation energies of $Li_5La_3Nb_2O_{12}$ and $Li_5La_3Ta_2O_{12}$ for ionic conductivity are 0.43 eV and 0.56 eV, respectively.[32] The ion conductivity of $Li_5La_3M_2O_{12}$ (M = Nb, Ta) could be improved by the substitution of La with low-valence ions (Ca, Sr, Ba).[33–35] Among these substituted $Li_6ALa_2M_2O_{12}$ (A = Ca, Sr, Ba) materials, $Li_6BaLa_2Ta_2O_{12}$ possesses the highest conductivity, 4×10^{-5} S·cm^{-1}, and the lowest activation energy, 0.40 eV. Besides La replacement, M (M = Nb, Ta) has also been replaced by In or Zr. $Li_{5.5}La_3Nb_{1.75}In_{0.25}O_{12}$ exhibits a conductivity of 1.8×10^{-4} S·cm^{-1} at 50 °C. Weppner *et al.* synthesized cubic-structure $Li_7La_3Zr_2O_{12}$ in 2007, which has the highest conductivity of 3×10^{-4} S·cm^{-1} and the lowest activation energy of 0.3 eV for garnet structure materials.[36] By contrast, tetragonal structure $Li_7La_3Zr_2O_{12}$ has the bulk Li^+-ion conductivity of 1.63×10^{-6} S·cm^{-1} and the grain-boundary Li^+-ion conductivity of 5.59×10^{-7} S·cm^{-1} at 300 K with a high activation energy of 0.54 eV in the temperature range of 300–560 K.[37] They explained the large difference in conductivity by considering order–disorder arrangements. The tetrahedral and octahedral sites are completely ordered by Li atoms and vacancies in tetragonal $Li_7La_3Zr_2O_{12}$, while the cubic $Li_7La_3Zr_2O_{12}$ shows a complicated Li-vacancy disordering on the tetrahedral and octahedral sites.[37] The tetrahedral structure is stable at RT, and transforms into a cubic structure between 100 °C and 150 °C. However, the high-temperature cubic phase could be made stable at RT by Al doping, which arises from the distress of Al_2O_3 during the reaction process.[38]

The conductivity of $Li_7La_3Zr_2O_{12}$ could be further enhanced by the substitution of other metals for Zr. Murugan *et al.* synthesized cubic $Li_{7.06}La_3Y_{0.06}Zr_{1.94}O_{12}$ with a conductivity of 8.1×10^{-4} S·cm^{-1} at RT.[39] The replacements of La^{4+} with Ta^{5+} or Nb^{5+} could also increase the conductivity over 8×10^{-4} S·cm^{-1}, and the activation energy is 0.22–0.35 eV.[40–42] The highest conductivity of garnet-structure compounds is obtained in $Li_{6.5}La_3Zr_{1.75}Te_{0.25}O_{12}$, which reaches 1.02×10^{-3} S·cm^{-1} at RT.[43]

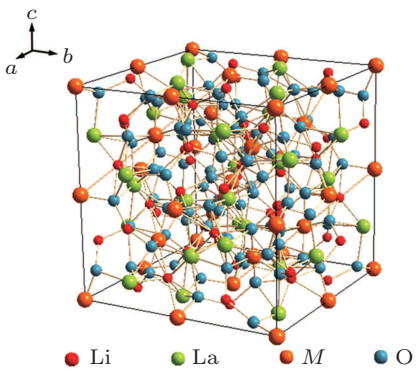


Fig. 6. Structure schematic of $Li_5La_3M_2O_{12}$ (M=Nb, Ta).

2.2. Sulfide solid electrolytes

2.2.1. Li_2S–SiS_2 system

Kennedy was the first to synthesize the Li_2S–SiS_2 solid electrolyte in 1986, using a melting-quench method. It exhibited ion conductivity in the range of 10^{-6} to 10^{-3} S·cm^{-1}.[44,45] Anhydrous Li_2S and SiS_2 were fixed with a molar ratio of 3:2, and the mixture was doped with LiI and calcinated at 950 °C for 1 h in Ar atmosphere. The composition of $0.6(0.4SiS_2–0.6Li_2S)–0.4LiI$ was found to exhibit the highest conductivity, 1.8×10^{-3} S·cm^{-1}, with activation energy of 0.28 eV. Since then, Li_2S–SiS_2 based glass electrolytes have been widely investigated to improve the ion conductivity and electrochemical stability.[46–49] Morimoto *et al.* prepared amorphous Li_2S–SiS_2 by high-energy ball milling.[50] Samples exhibited conductivity of 1.5×10^{-4} S·cm^{-1}. Kondo *et al.* reported the Li_2S–SiS_2 system doped with Li_3PO_4, which exhibited a conductivity of 6.9×10^{-4} S·cm^{-1}, and stability with regard to electrochemical reduction was highly superior.[48]

2.2.2. Li_2S–P_2S_5 system

A new crystalline material family, lithium superionic conductors (*thio*-LISICON), was found in the Li_2S–GeS_2–P_2S_5 system by Murayama *et al.* in 2001.[51] The *thio*-LISICON structure of $Li_{4-x}Ge_{1-x}P_xS_4$ is classified into three regions: region I: $(0 < x \leq 0.6)$, region II: $(0.6 < x < 0.8)$, and region III: $(0.8 \leq x < 1.0)$, as shown in Fig. 7.

Due to their high ionic conductivity, Li_2S–P_2S_5 system lithium ion conductors are extensively studied. Actually, the conductivity of Li_2S–P_2S_5 stable phases prepared from solid phase reaction is very low.[52] However, the Li_2S–P_2S_5 amorphous phases prepared by mechanical milling or melt quenching exhibit higher conductivity, and the conductivity of the Li_2S–P_2S_5 system could be further improved with the formation of crystalline phases by glass crystallization.[52,53] The enhancement of Li^+-ion conductivity in the glass-ceramics is attributed to the precipitation of the meta-stable crystalline phase.[53] $80Li_2S–20P_2S_5$ (mol%) and $75Li_2S–25P_2S_5$ (mol%) were prepared by high-energy ball-milling and subsequent heat-treatment.[54] The conductivity of $80Li_2S–20P_2S_5$ (mol%) reached around 10^{-3} S·cm^{-1}.[55] The composition $75Li_2S–25P_2S_5$ (mol%) could exhibit several structures depending on the preparation conditions. Li_3PS_4 has been prepared by high-temperature solid reaction.[56] β-Li_3PS_4 was obtained above 190 °C, and transformed to γ-Li_3PS_4 below 190 °C.[56] β-Li_3PS_4 is a highly ion conductive phase, while γ-Li_3PS_4 is a low ion conductive phase. However, the high-temperature phase β-Li_3PS_4 can be stable at RT with a porous structure.[57] The conductivity of β-Li_3PS_4 is about 1.6×10^{-4} S·cm^{-1} and could be improved to 6.3×10^{-4} S·cm^{-1} with LiI doping to form a new phase of $Li_7P_2S_8I$.[58] Moreover, the conductivity of *thio*-LISICON structure Li_3PS_4 could reach 1.0×10^{-3} S·cm^{-1}.[59]

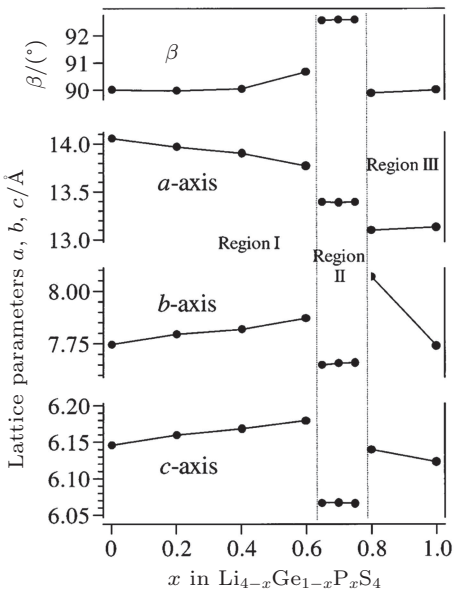


Fig. 7. Composition dependence of lattice parameters in $Li_{4-x}Ge_{1-x}P_xS_4$, determined by XRD measurements. The lattice parameters plotted in the figure are based on the parent lattice of the LISICON with $a \times b \times c$ cells.[51]

However, the chemical stability of the Li_2S–P_2S_5 system is low, and the system is prone to react with moisture to generate H_2S gas.[60,61] The substitution of oxides in Li_2S–P_2S_5 was observed to increase its chemical stability.[61] Furthermore, the presence of oxygen atoms in Li_2S–P_2S_5 was reported to decrease the interface resistance between oxide electrodes and sulfide electrolytes.[62,63] The Li^+-ion conductivity of $70Li_2S–30P_2S_5$ could be further improved by oxide substitution.[64] Minami *et al.* reported on a $70Li_2S–30P_2S_5$ system with P_2S_3 and P_2O_5 substituted, respectively.[64] When P_2S_3 was substituted, the glass-ceramics with 1 mol% P_2S_3 exhibited the highest conductivity, and the conductivity increased 29% compared with the pristine sample.[64] When P_2O_5 was substituted, the highest conductivity was obtained at a substitution amount of 3% P_2O_5, and the conductivity increased 10% compared with the pristine sample. The substitution effects of Li_3PO_4 are similar to those of P_2S_3, which could be related to their complex substitution mechanism.[47] Moreover, the meta-stable phase $Li_7P_3S_{11}$ has the highest conductivity of 3.2×10^{-3} S·cm^{-1} in the $70Li_2S–30P_2S_5$ system.[52] Recently, Seino *et al.* prepared meta-stable phase $Li_7P_3S_{11}$ by hot pressing, and the conductivity was as high as 1.7×10^{-2} S·cm^{-1}.[65]

Recently, a new structure, $Li_{10}GeP_2S_{12}$ (Fig. 8) was first synthesized in 2011; it has an extremely high ionic conductivity of 1.2×10^{-2} S·cm^{-1}.[66] The discovery of the new structure $Li_{10}GeP_2S_{12}$ electrolyte resulted in a wide range of fundamental studies on ionic mobility in bulk materials and

promoted the development of next-generation batteries.[59,67] However, since Ge is very expensive, Roling *et al*. synthesized $Li_{10}SnP_2S_{12}$, replacing Ge with Sn.[68] Although the RT conductivity of $Li_{10}SnP_2S_{12}$ is only 4×10^{-3} S·cm^{-1}, obviously lower than that of $Li_{10}GeP_2S_{12}$, the cost of the raw materials is reduced by a factor of ~ 3.

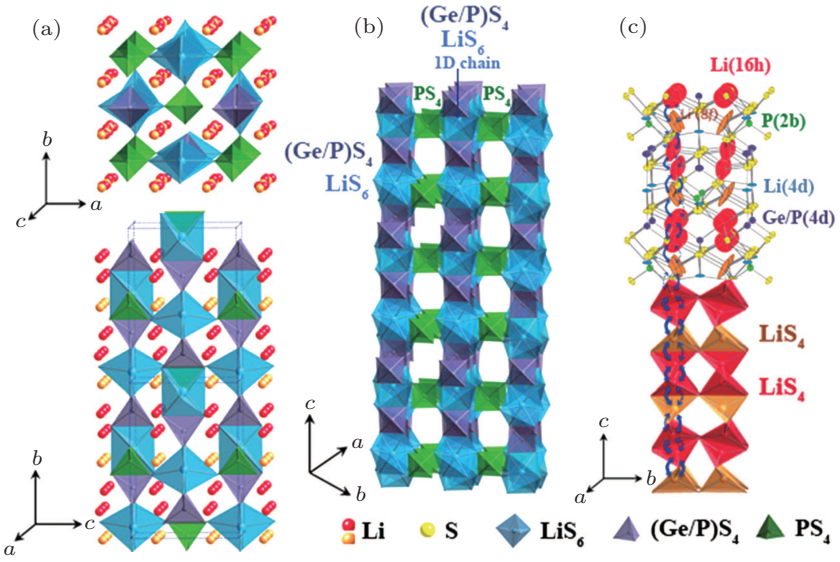


Fig. 8. Crystal structure of $Li_{10}GeP_2S_{12}$. (a) The framework structure and lithium ions that participate in ionic conduction. (b) Framework structure of $Li_{10}GeP_2S_{12}$. (c) Conduction pathways of Li^+ ions.[66]

3. Electrode materials for all-solid-state lithium batteries

3.1. Cathode materials

The specific capacity of cathode materials currently in use is less than half that of negative electrode materials. Therefore, high-capacity cathode materials are necessary for lithium-ion batteries with higher energy densities. The most commonly used cathode materials in all-solid-state lithium batteries can be classified into two categories based on the cell potential.[69] One is lithium transition-metal oxides, with a potential of 3.5–5 V, which are considered to be viable candidates for ASSLiBs because of their highly reversible intercalation/deintercalation reaction and high operating potential. They include $LiCoO_2$,[70] $LiNiO_2$,[71] $LiNi_{0.8}Co_{0.15}Al_{0.05}O_2$,[72] $LiNi_{0.33}Co_{0.33}Mn_{0.33}O_2$,[73] $LiMn_2O_4$,[74] and $LiNi_{0.5}Mn_{1.5}O_4$.[75] The other one is sulfur-based materials (S and Li_2S) and metal sulfides (M_xS_y, M generally being a transitional metal) with a potential below 3.0 V, such as Li_2S,[76] Li_2S–C,[77] S–C,[78] Li_2S–Cu,[79] TiS_2,[80] FeS,[81] FeS_2,[82] and NiS.[83,84]

3.1.1. Lithium transition-metal oxides

Lithium cobalt oxide Layered $LiCoO_2$ was the first commercialized cathode material used in the traditional LiBs, and it is also widely studied in ASSLiBs. Bare $LiCoO_2$ in ASSLiBs generally suffers from small energy density and low rate capability, due to the large interfacial resistance caused by the space-charge layer effect,[12,85] structural degradation originating from mutual diffusion of elements,[86,87] or poor electrode/solid electrolyte (SE) interface contact.[70,88] Takada *et al*. pointed out that electron-insulating and ion-conducting oxide materials ($LiNbO_3$,[89] $Li_4Ti_5O_{12}$,[12] TaO_3[62]) as a nanoscale coating layer on $LiCoO_2$ could suppress the formation of a space charge layer and notably improve the power density of $LiCoO_2$. Further, Xu *et al.* reported an easy way to construct the buffer layer with low electronic conduction by post-annealing. Their results indicate that a self-formed buffer layer with Al element enrichment on the surface of $LiAl_xCo_{1-x}O_2$ particles also could suppress the formation of a space charge layer.[63] Oxide coatings also improve the high-voltage performance of $LiCoO_2$ in ASSLiBs by suppressing the interfacial resistance between $LiCoO_2$ and SEs at a high cutoff voltage of 4.6 V (vs. Li/Li$^+$) (Fig. 9),[90] which could further enhance the energy density of ASSLiBs. In addition, Tatsumisago *et al*. reported that $LiCoO_2$ coated with electronic conductive coatings such as NiS or CoS could also improve the electrochemical performance of $LiCoO_2$.[87] They ascribed the poor performance of bare $LiCoO_2$ to structural degradation originating from mutual diffusion of elements at the interface[86,87] rather than the space charge layer. Besides, Woo *et al.* reported that a uniform nanoscale Al_2O_3 layer deposited on $LiCoO_2$ by atomic layer deposition could also benefit the cyclic performance of ASSLiB by reducing the formation of an interfacial layer.[91]

In addition, coating SE on $LiCoO_2$ particles by pulsed laser deposition[70,88] or *in situ* wet coating in solution[92,93] is

a direct way to improve the lithium-ion conducting paths between electrode and SEs. $LiCoO_2$ coated with Li_2S–P_2S_5 SE by pulsed laser deposition showed a stable reversible capacity of 133 mA·h·g^{-1} for use as a cathode in the all-solid-state cell.[70] However, the effect of wet coating SE on $LiCoO_2$ was limited, due to the low conductivity and unevenness of the SE coating layer.[92,93]

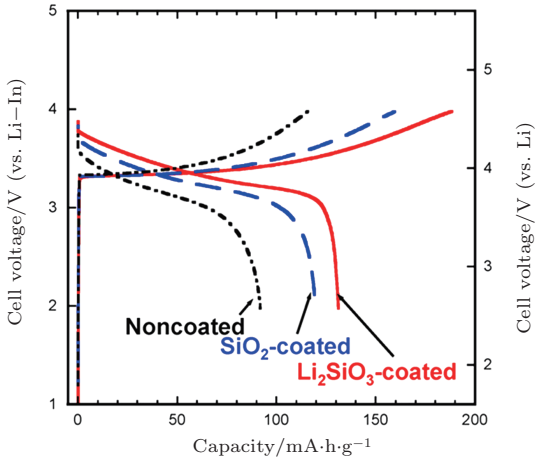


Fig. 9. Charge–discharge curves of all-solid-state cells, In/80Li_2S–20P_2S_5 glass-ceramic/$LiCoO_2$ with uncoated, SiO_2-coated, and Li_2SiO_3-coated $LiCoO_2$. The current density and cutoff voltage are 0.13 mA·cm^{-2} and 4.6 V (vs. Li), respectively.[90]

Lithium nickel cobalt manganese oxide First reported by Ohzuku *et al.*, $LiNi_{1/3}Co_{1/3}Mn_{1/3}O_2$ is a very attractive cathode material for conventional LiBs because of its high capacity and good cyclic performance.[94] Among all the Li–Ni–Co–Mn oxide positive electrode materials, bare $LiNi_{1/3}Co_{1/3}Mn_{1/3}O_2$ showed the highest discharge capacity and capacity retention in ASSLiBs using the sulfide-based SE.[71] The Li–In/$Li_{10}GeP_2S_{12}$/$LiNi_{1/3}Co_{1/3}Mn_{1/3}$ battery developed in our group[95] showed results similar to those reported by Kitaura *et al.*,[71] exhibiting initial charge/discharge capacities of 150.3/114.5 mA·h·g^{-1} at a current density of 0.11 mA·cm^{-2} between 2.0 V and 3.68 V (vs. Li–In). Recently, $LiNi_{1/3}Co_{1/3}Mn_{1/3}O_2$ surfaces modified with coating layers presented promising performance in ASSLiBs.[73,96–98] Iwasaki[73] first coated $LiNi_{1/3}Co_{1/3}Mn_{1/3}O_2$ with $LiNbO_3$, followed by depositing a thick, dense film on the LATP Li^+-conductive glass-ceramic sheets. As a result, the obtained ASSLiB of Li/LiPON/LATP-sheet/NCM-composite-film/Pt showed a discharge capacity of 152 mA·h·g^{-1} (3.0–4.2 V, 0.025 C, 333 K) and cycled for 20 cycles. Similar to $LiCoO_2$ cathodes, the oxide coating layers are effective in decreasing the interfacial resistance between $LiNi_{1/3}Co_{1/3}Mn_{1/3}O_2$ and the sulfide-based solid electrolyte. $LiAlO_2$-coated $LiNi_{1/3}Mn_{1/3}Co_{1/3}O_2$ electrode assembled with amorphous solid electrolytes Li_3PS_4 showed an initial discharge capacity of 134 mA·h·g^{-1} and retained a capacity of more than 124 mA·h·g^{-1} even after 400 charge-discharge cycles at a current density of 11 mA·g^{-1}.[97]

Aluminum-doped lithium nickel cobalt oxide Ni-based cathode material $LiNi_{0.8}Co_{0.15}Al_{0.05}O_2$ (NCA) is regarded as a promising cathode in ASSLiBs because of its higher capacity, higher rate capability, and lower toxicity compared to $LiCoO_2$ cathodes.[72] The pristine NCA in ASSLiBs with 80Li_2S–20P_2S_5 SE exhibited a large interfacial resistance, partly due to the surface-adsorbed carbonate impurities. Heating NCA powder at 250 °C in a vacuum could eliminate the obstacle of charge transfer at the cathode/SE interface and improve the initial capacity.[99] Besides the surface impurities, the highly developed space-charge layer at the interface of NCA and SE is the main reason for the high interfacial resistance. Similar to $LiCoO_2$, a thin buffer layer of $Li_4Ti_5O_{12}$,[72] $LiNbO_3$,[100] or Li_2O–ZrO_2[101] coated on NCA can suppress the formation of high-resistance layers. An ASSLiB of In/70Li_2S–30P_2S_5/$Li_4Ti_5O_{12}$-coated NCA exhibited discharge capacities of 150 mA·h·g^{-1} and 110 mA·h·g^{-1} at current densities of 0.5 mA·cm^{-2} and 10 mA·cm^{-2}, respectively (1.5–3.6 V, 25 °C), somewhat higher than those of $LiCoO_2$.[72] Recently, Ito *et al.* fabricated a 1 A·h class pure solid state battery with Li_2O–ZrO_2 coated NCA as the cathode. The battery retained 80% capacity after 100 cycles (0.1 C, 25 °C). Although the cell performance is still not sufficient for EV applications, this achievement indicates the feasibility of NCA cathodes in bulk-type ASSLiBs.[101]

Lithium manganese oxide Besides the layered-structure lithium transition metal oxides, spinel structured $LiMn_2O_4$ is another important cathode material for lithium-ion batteries. $LiMn_2O_4$ as a cathode in an ASSLiB exhibited a lower discharge capacity, but smaller irreversible capacity and better cycle performance than those of other lithium transition-metal oxide cathodes.[71] All-solid-state In/$LiMn_2O_4$ cells with 80Li_2S–20P_2S_5 as solid electrolyte[74] showed an initial discharge capacity of 55 mA·h·g^{-1} at a current density of 0.064 mA·cm^{-2} (2.4–4.6 V vs. Li/Li^+). After the charge process, the interfacial resistance between the $LiMn_2O_4$ electrode and the solid electrolyte was identified, possibly caused by the reaction between $LiMn_2O_4$ and the solid electrolytes or by decomposition of $LiMn_2O_4$ during cycling. Coating techniques for $LiMn_2O_4$ are effective in suppressing the Mn diffusion in ASSLiB. The interfacial resistance between $LiMn_2O_4$ and the electrolyte decreased when the $LiMn_2O_4$ particles were coated with amorphous $Li_4Ti_5O_{12}$. A higher discharge capacity was obtained in the cell with lithium-titanate-coated $LiMn_2O_4$ than that with uncoated $LiMn_2O_4$ at current densities in the range of 0.064 to 2.6 mA·cm^{-2}.[102]

3.1.2. Sulfur-based materials (S and Li_2S) and metal sulfides (M_xS_y)

In order to improve the energy density of ASSLiBs, utilization of active materials with high capacity is effective. Sul-

fur and lithium sulfide are regarded as promising cathode materials for lithium batteries due to their high theoretical capacities of 1672 mA·h·g^{-1} and 1168 mA·h·g^{-1}, respectively.[103] However, the two major limitations of these two materials are the essential low electronic and Li^+-ion conductivities, and capacity fading because of high dissolution of lithium polysulfide into the liquid electrolyte during the electrochemical reactions.[104] Formation of nanocomposites of sulfur or Li_2S with various forms of carbon is a useful strategy to improve the electronic conductivity. These nano-sized active particles could simultaneously provide short diffusion lengths for Li^+ ions.[77] As to the issue of solubility of the lithium polysulfides, replacing the traditional liquid electrolytes with inorganic SEs seems to be effective. Sulfur-based materials or metal sulfides could be employed as cathodes for ASSLiBs due to their good interface compatibility with sulfide-based solid-state electrolytes and mild operating voltages.[105]

Tatsumisago's group reported a series of S-nanocarbon and Li_2S-nanocarbon composites as cathode materials in all-solid-state cells using Li_2S–P_2S_5 as SE.[77,79,106] The sulfur or Li_2S cathodes for all-solid batteries were prepared primarily by high-energy mixing or ball-milling of sulfur-based materials with conductive carbons and solid electrolytes. The smooth and adhesive interface among the three components can be realized at nanoscale by mechanical milling. For example, the composite cathode prepared by ball milling a mixture of sulfur, activated carbon, and amorphous SE of $Li_{1.5}PS_{3.3}$ exhibited a reversible capacity as high as 1600 mA·h·g^{-1} after 100 cycles at 1 C current density at 25 °C (Fig. 10).[107] The *ex situ* sulfur *K*-edge x-ray absorption fine structure measurements suggested that the ideal electrochemical reaction $Li_2S \leftrightarrow 2\,Li + S$ proceeded in the ASSLiB, probably due to the suppression of the formation of polysulfides in the electrolyte.[108] Lithium sulfide as a prelithiated cathode is an ideal high capacity electrode material for ASSLiBs, the use of which avoids the direct use of metallic lithium as the anode. Recently, Nagao *et al.* found that Li_2S electrodes prepared by high-energy planetary ball milling exhibited excellent cycling stability with high capacity of 700 mA·h·g^{-1} in ASSLiBs.[77] They further investigated the reaction mechanism of Li_2S electrodes, the morphology and structure of reaction products in ASSLiBs. It was found that all Li_2S particles changed completely to amorphous sulfur during the first charge process. However, at the first discharge process, amorphous sulfur derived from Li_2S nanoparticles with sizes less than 10 nm formed crystalline Li_2S, while S derived from Li_2S with a larger size resulted in intermediate crystalline Li_2S_x, which caused a large initial irreversible capacity.[76] Therefore, the formation of a continuous and intimate solid-solid interface between electrolyte and electrode and the miniaturization of the active particles at nanoscale are important to the realization of the high energy density and excellent cycling stability of sulfur-based ASSLiBs. Lin *et al.* also pointed out that the reduction of particle size improves the ionic conductivity of nano Li_2S by two orders of magnitude compared to the bulk Li_2S. Moreover, the ionic conductivity of nano Li_2S can be further improved by four orders of magnitude by forming a core–shell structure of nano Li_2S@Li_3PS_4. Excellent cyclability and rate capability of this nano Li_2S coated with high ionic-conductive Li_3PS_4 were realized in ASSLiBs.[109]

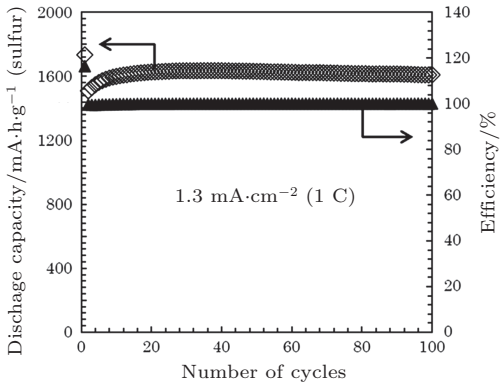


Fig. 10. Cycling performance of all-solid-state lithium sulfur (Li/S) cell containing an AC-based positive composite electrode, at 1.3 mA·cm^{-2} (1 C) at 25 °C. The weight of the positive composite electrode is 1.2 mg. The cut-off voltage is kept between 0.5 V and 2.5 V (vs. Li–In).[107]

Compared to sulfur or Li_2S, metal sulfide nanoparticles or nanocomposites of carbon with metal sulfides, such as FeS,[81] TiS_2,[80] NiS,[83] NiS-VGCF (vapor grown carbon fiber),[84] Mo_6S_8, and $Cu_xMo_6S_{8-y}$[110] have similar interfacial stability and high capacity with sulfur-based solid electrolytes. Moreover, they exhibit better rate capability and cyclability because of relatively higher electronic conductivity. For example, NiS nanoparticles synthesized in high-boiling solvents exhibited a large capacity of 680 mA·h·g^{-1} after 20 cycles at 0.13 mA·cm^{-2}.[83] To improve the rate capability of ASSLiBs, NiS-VGCF-SE composites were prepared by coating the electrolyte $80Li_2S{\cdot}20P_2S_5$ onto the NiS-VGCF composite using pulsed laser deposition to form continuous lithium-ion and electron conduction paths for the NiS active material. As a result, NiS-VGCF-SE composite showed a reversible capacity of 430 mA·h·g^{-1} at a higher current density of 1.3 mA·cm^{-2}.[84]

3.1.3. Anode materials

Lithium metal In theory, ASSLiBs with inorganic solid state electrolytes free from flammable components and having high mechanical strength can incorporate lithium metal as an anode and take advantage of maximizing its energy density. However, the internal short circuits caused by abnormal lithium dendritic growth and the electrochemical reaction of the SEs with lithium metal both limit the application of lithium metal anodes. Nagao *et al.* found that lithium metal tends to grow in the voids and along the grain boundaries of $Li_2S{\cdot}P_2S_5$

SE pellets during cycling in a bulk-type solid-state cell.[111] Shin *et al*. reported that the structure of Li_2S–GeS_2–P_2S_5 is severely changed at low voltage ranges because of the reduction of element Ge.[59] The poor chemical stability of the SE in contact with lithium is also found in Li_4SnS_4 because of the reduction of tin. In order to address this issue, modifying the surface of the electrolyte or passivating the Li electrode to achieve good compatibility with metallic lithium has been tried. The $3LiBH_4$·LiI is a viable protective coating layer on Li_4SnS_4 to improve its compatibility with lithium electrodes.[112] Modifying the surface of metallic lithium by N_2 gas can suppress the side reaction between Li_3PO_4–Li_2S–SiS_2 SE and lithium metal electrode.[113] It seems that using lithium metal as the anode material in ASSLiBs will remain a challenge unless significant progress is made in electrolyte composition, surface modification, and pelletized microstructure of SEs, or an effective protective layer on Li foil is achieved.

Lithium alloys Lithium alloys (e.g., Li–In, Li–Si, Li–Al) anodes are good alternatives to replace lithium metal in ASSLiBs, owing to their safety and high capacity. Lithium-alloy anodes have a charge/discharge mechanism involving alloying and de-alloying ($xLi^+ + xe^- + M \leftrightarrow Li_xM$). Among these alloys, Li–In alloy has a flat voltage plateau at 0.62 V (vs. Li/Li^+) for Li_xIn ($0 < x < 1$), fast charge transfer kinetics, and reversible electrochemical reaction.[114,115] The relatively high working voltage of Li–In anode can efficiently avoid the deformation of SEs. As a result, Li–In alloy is the most commonly used anode in ASSLiBs.[70,72,84,106]

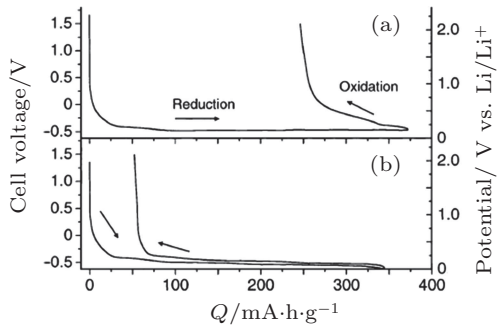


Fig. 11. Discharge–charge curves of the cell, Li–In/graphite using Li_3PO_4–Li_2S–SiS_2 glass (a) and LiI–Li_2S–P_2S_5 (b) as electrolyte. The right vertical axis shows the potential of the working electrode vs. Li/Li^+ calculated by adding the potential of the counter electrode (0.62 V vs. Li/Li^+) to the cell voltage.[118]

Graphite Graphite, having a low Li^+-ion intercalation/deintercalation potential plateau, below 0.2 V (vs. Li/Li^+), and theoretical capacity of 372 mA·h·g^{-1}, has been successfully used as anodes in commercial LiBs. It is also a possible anode material for ASSLiBs with sulfur-based SEs. Graphite exhibits high reversibility in ASSLiBs with Li_2S_5–P_2S_5[99,101,116,117] and LiI–Li_2S–P_2S_5[118] as SEs. However, some SEs tend toward electrochemical reduction when in contact with graphite at low potential[118,119] Li_2S–GeS_2–P_2S_5 with high Li^+-ion conductivity is not compatible with graphite because of the reduction of SEs. Takada pointed out that this is probably due to the reduction of GeS_2.[118] Similarly, the Li_3PO_4–Li_2S–SiS_2 system goes through an irreversible reaction because of the reduction of SiS_2.[118] The reduction of electrolyte at the surface of graphite causes a large irreversible initial capacity of ASSLiBs (Fig. 11).

4. Electrolyte/electrode interface phenomena

The basic problem of all solid–state lithium batteries is their low power density, which results from the large charge transfer resistance at the interface between the electrode and the solid electrolyte. In addition, the rate capability, coulombic efficiency,[120] and cycle stability are also closely related with the interface.[59,121] Electrochemical impedance spectroscopy (EIS) is a powerful tool to characterize the interfacial resistance in ASSLiBs.[75,86,105] Hayashi *et al.* systematically investigated the interface of In/ Li_2S–P_2S_5/$LiCoO_2$ cell in ASSLiBs with EIS, finding that the impedance profile at the charge state is composed of one intercept point in the high frequency region and two semicircles in the medium and low frequency regions, corresponding to the resistance of the solid electrolyte layer, the resistance in the positive electrode layer (interfacial resistance between $LiCoO_2$ and Li_2S–P_2S_5 solid electrolyte) and the negative electrode layer, respectively.[86] The interfacial resistance in the electrode layers accounts for more than 60% of the total resistances. Hence, in order to improve the low rate capability, high overpotential, and large initial irreversible capacity of ASSLiBs, it is necessary to reduce the total resistances of the cell. In particular, improvement of the properties of electrode/electrolytes interfaces would engender a low interfacial resistance and improve the electrochemical performance of ASSLiBs. Specifically, the main challenges inherent in the interface between an electrode and a solid electrolyte are: (i) small contact area, (ii) side reactions by element co-diffusion, (iii) impediment of ion diffusion by space charge layer, and (iv) interface stress induced by volume changes.

4.1. Contact area between electrolyte and electrode

Formation of a favorable solid–solid interface between electrode and electrolyte is crucial to achieve excellent performance in solid-state batteries.[69,122] Two useful tactics are mechano-chemical preparation of nanocomposite electrodes and formation of electrolyte on active material by softening the electrolyte or by pulsed laser deposition coating, as shown in Fig. 12.[69]

For the nanocomposite electrodes, the mixture process has an obvious effect on the capacity, and the complete mixture benefits the capacity by increasing the contact area between electrode and electrolyte.[123] The nanocomposite elec-

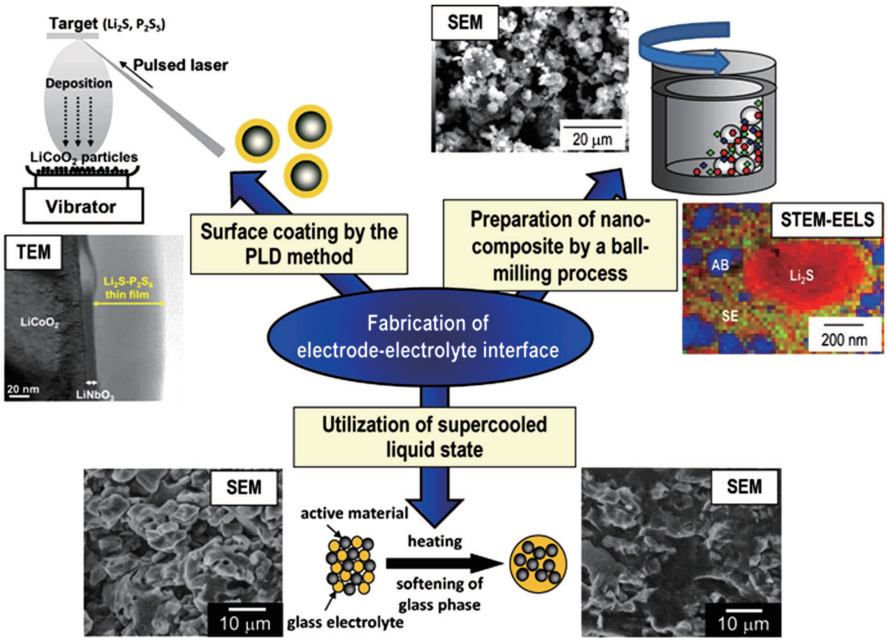


Fig. 12. Schematic of several approaches to form good electrode/electrolyte interfaces.[69]

trodes can be prepared by ball-milling, which not only increases the contact area[77] but also induces the formation of an amorphous interface layer to enhance the capacity.[80,124] Nanocrystalization of electrodes can also effectively improve their rate capability.[109,125] In addition, a favorable solid–solid interface can be prepared by softening sulfide glass electrolyte at its glass transition temperature.[126] Besides, the coating of a highly conductive SE on active material particles is a promising technique to form an effective electrode–electrolyte interface and a lithium-ion conducting path in the composite.[88]

4.2. Interface diffusion

Sakuda *et al*. characterized the interface of $LiCoO_2$ and Li_2S–P_2S_5 with transmission electron microscopy and observed mutual diffusions of Co, P, and S at the interface.[86] They proposed that an interfacial CoS layer is formed during the charge–discharge process, resulting in the increase of interface resistance and therefore decreasing the discharge capacity.[127] A Li_2SiO_3 buffer layer could improve cycle stability and high-rate performances by hindering element diffusions.[128] To justify this assumption, they coated $LiCoO_2$ with CoS and NiS respectively, and found that the interface resistance is reduced by each of these coatings, which implies that the presence of a thin CoS layer is not the cause of the large interfacial resistance between $LiCoO_2$ and Li_2S–P_2S_5. Thus, degradation of the solid electrolyte and/or the $LiCoO_2$ electrode at the interface is considered to be the main cause of the large interfacial resistance. Thin CoS and NiS coatings act as buffer layers that suppress degradation at the highly reactive interface between charged $LiCoO_2$ and Li_2S–P_2S_5 solid electrolyte.[87] Besides electron-conductive metal sulfides, ion-conducting oxide materials, such as $LiNbO_3$,[89,100] Li_2O–ZrO_2,[101] Li_2O–SiO_2,[128] $Li_4Ti_5O_{12}$,[12,72] and TaO_3,[62] were also coated on oxide cathode materials by a wet-chemical method or atomic layer deposition in order to suppress the chemical reactions between the sulfide electrolytes and the oxide cathodes. Similar interface diffusion is found between oxide electrolytes and oxide cathodes, and the similar surface coating modification of Nb layer was chosen to reduce this interfacial resistance.[129,130]

4.3. Space-charge layer

For the interface between an oxide electrode and a sulfide solid electrolyte, Takada *et al*. attributed the rate-determining step of the battery reactions to ionic transport at the interface rather than bulk in the battery components.[7,12,72,89,131,132] They assumed that only Li^+ ions are mobile in the all-solid-state lithium batteries, with no side reaction at the interface.[7] Ionic conductors often exhibit anomalous transport properties at their surface or at their interface with various other materials. Such phenomena are attributed to a space-charge layer at the surface or the interface that has different mobile-ion concentration from the bulk, as shown in Fig. 13. Since the thickness of the space-charge layer is around 10 nm, such anomalous ionic conduction is considered to be an example of nanoionics.[133] To be specific, depletion of lithium in the sulfide SE side is triggered by the large difference of Li^+-ion chemical potential between the oxide cathode and the sulfide electrolyte. Because the high potential of the cathodes depletes the lithium ions, such high resistance will not be found at the anode/electrolyte interfaces, which also could explain the low

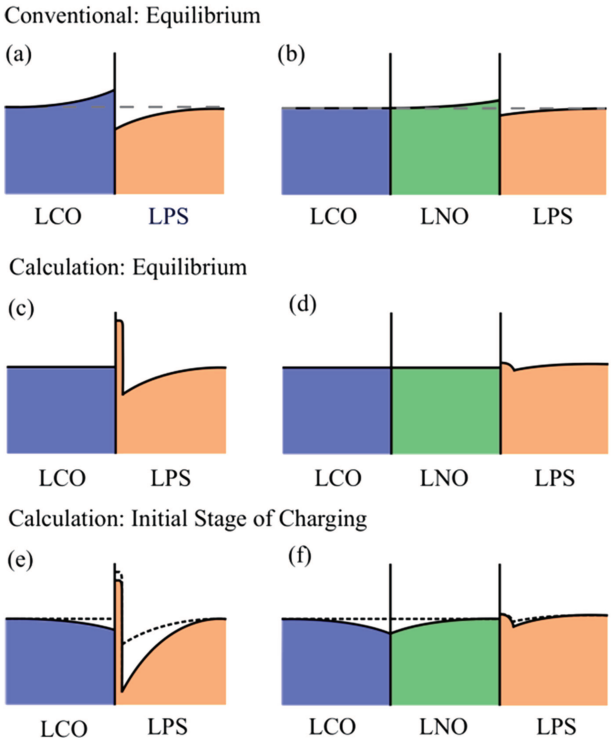


Fig. 13. Schematic illustrations of interfacial Li concentration. The equilibrium concentrations expected by the conventional model and indicated by the present calculations for the LCO/LPS interface ((a) and (c)) as well as the LCO/LNO/LPS ((b) and (d)). The Li concentrations in panels (e) and (f) describe the expected changes at the initial stage of charging for both interfaces proposed in the calculation.[85]

resistance at the interface of a sulfide electrolyte and a sulfide electrode. Takada *et al.* suggested the existence of a space-charge layer, evidenced by the potential slope at the initial stage of charging in the voltage profile. Subsequently, the distribution of lithium ions was calculated by computer modeling, which further proved the existence of a space-charge layer.[85] They pointed out that one way to reduce the interfacial resistance is introducing a buffer layer to shield the sulfide solid electrolyte from the high potential of the oxide cathode. The surface coating suppresses the formation of a lithium-depleted layer at the interface to reduce the resistance. The layer interposed between the oxide electrode and the electrolyte should have the following characteristics: anions of buffer layer materials with large electronegativity and lithium-ion conductor but electron insulator. An amorphous oxide lithium-ion conductor would be a good candidate for the buffer layer.[12,62,89,97,100] Takada *et al.* also investigated the influence of the thickness of the coating layer on the interfacial resistance by EIS.[7,12] The results indicated that the interfacial resistance of $LiCoO_2$coated by an $Li_4Ti_5O_{12}$ layer with a thickness of 5 nm was 20 times smaller than that for uncoated $LiCoO_2$, and the rate capability of the ASSLiB was improved effectively. Space-charge layers also exist between oxide electrodes and oxide electrolytes, and a Li depletion layer or accumulation layer can form depending on the chemical potential of electrode and electrolyte.[134] For example, $Li/Li_{3.2}PO_{3.8}N_{0.2}/LiCr_{0.05}Ni_{0.45}Mn_{1.5}O_{4-\delta}$ batteries showed poor electrochemical performance because of the huge resistance at the electrolyte/electrode interface caused by a large interface electric field generated by the large electric potential difference between electrolyte and electrode. However, the resistance was reduced by loading dielectric nanoparticles of $BaTiO_3$ on the surface of $LiCr_{0.05}Ni_{0.45}Mn_{1.5}O_{4-\delta}$. As a result, the $BaTiO_3$ nanoparticle-modified battery of $Li/Li_{3.2}PO_{3.8}N_{0.2}/LiCr_{0.05}Ni_{0.45}Mn_{1.5}O_{4-\delta}$ demonstrated an improved rate capability with discharge capacity of 100 $mA{\cdot}h{\cdot}g^{-1}$ at 8 C rate.[75]

4.4. Interface stress induced by electrode's volume changes

When $LiCoO_2$ is lithiated/delithiated, the volume of $LiCoO_2$ changes repeatedly. This change occurs uniformly throughout the electrode, including the interface. So the electrode-solid electrolyte interface is stressed by the change of $LiCoO_2$ volume, and the stress increases the local distortion at the electrode, increasing resistance for the charge transfer reaction. An oxide electrolyte buffer layer NbO_2 film is introduced between electrolytes and electrodes, which could effectively reduce the change of Co–O bonding, and thus decrease the interface stress.[130] As to the electrode materials with massive volume change during charge and discharge, such as S and Li_2S ($\sim$179% volumetric expansion during lithiation from S to Li_2S[80]), constructing a nanocomposite structure of sulfur or Li_2S is a good strategy to address the stress problem. The nano-size active materials could relieve the stresses induced by the volume during cycling. At the same time, carbon materials could act as a buffer phase to the volume change.[76,108] In film ASSLiBs, an effect of mismatch strain caused by the lattice expansion and contraction of electrode materials can cause high stress concentration along the interface, eventually yielding cracks around the interface. Introduction of amorphous layers with high ionic conductivity at the interface could suppress the interface separation as well as the consequent increase of the interfacial resistance.[135]

5. Fabrication and evaluation of all-solid-state lithium battery

In recent years, great progress has been made in ASSLiBs, mainly in addressing the electrode/electrolyte interface problems and elevating their energy and power densities.[69] A great many patents about all-solid-state lithium batteries have emerged, centering on preparation of the solid state electrolyte, surface modification technologies, and battery fabrication technologies.

Toyota Motors, for example, has been working on all-solid-state lithium batteries for many years and regards it as

a medium-term advanced battery solution. A prototype all-solid-state lithium battery, shown in Fig. 14, was unveiled in 2010. The prototype incorporates lithium cobalt dioxide ($LiCoO_2$), graphite, and sulfide as the positive electrode, negative electrode, and solid electrolyte, respectively. Four sets of positive electrode layers, solid electrolyte layers, and negative electrode layers are laminated, and the average voltage of the battery is 14.4 V (3.6 V×4). The battery can output a voltage of 16.26 V (4.065 V per layer) immediately after it is charged. In order to address the high interface resistance, a ceramic layer is coated on the surfaces of the positive electrode materials.

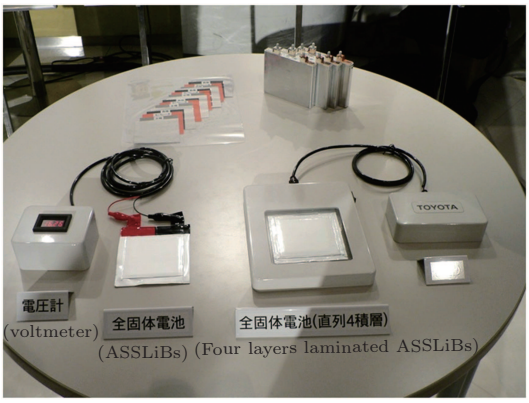


Fig. 14. Toyota Motors' all-solid-state lithium batteries.[136]

In addition, Idemitsu Kosan Co., Ltd. exhibited an A6-size laminated ASSLiB in 2010. The battery, with inorganic sulfide electrolytes, is safer and features high-temperature performance, resistance to overdischarge, and potentially higher energy density than the traditional LiBs with liquid electrolytes. The positive and negative electrodes in this prototype A6-size battery are the same as those of mainstream LiBs. The A6-size battery with cells connected in a series has an output voltage of 14–16 V. The solid electrolyte membrane used is about 100 μm thick. Idemitsu Kosan plans to reduce the thickness to 10–20 μm to lower the resistance and is searching for electrode materials that are compatible with the electrolyte. And, in theory, it is possible to increase the gravimetric energy density to 300 W·h/kg.

Samsung R&D Institute Japan, in cooperation with Samsung Electronics Co., Ltd., developed a 1 A·h class ASSLiB using a Li_2O–ZrO_2-coated NCA cathode, an artificial graphite anode, and a sulfide based electrolyte ($80\%Li_2S$–$20\%P_2S_5$) in 2014.[101] The standard-type single cells are fabricated by the wet printing method, and the 1 A·h class all-solid-state battery consists of three parallel stacks of the single cells. The interface resistance between NCA and sulfides is significantly reduced by the Li_2O–ZrO_2 coating, and the total cell resistance is approximately one quarter that of a cell without the coating. The battery displays 82% and 85% capacity retention after 100 cycles at 25 °C and 60 °C without any artificial external pressure, which convincingly demonstrates the high temperature stability of the all-solid-state battery. In subsequent work,[137] the electrochemical performance of large size ASSLiBs was further improved by using sulfide electrolyte with high ionic conductivity and thinner electrolyte layers, as well as an optimized fabrication process.

Recently, interesting results have been obtained in our group regarding the development of all-solid-state lithium batteries, including cathode materials, inorganic solid state electrolytes, and surface modification between electrode and electrolyte.[1,24] All-solid-state lithium batteries with A·h-class capacity have been successfully prepared by direct cold pressing using sulfide electrolytes and surface-modified $LiCoO_2$-based cathodes. The cathode delivered a discharge-specific capacity of 120 $mA{\cdot}h{\cdot}g^{-1}$, almost as high as that of the traditional LiBs. The interface resistance has been reduced to 8 $m\Omega{\cdot}cm^{-2}$, which is on the same level as Toyota Motors' prototypes.

6. Conclusions and perspectives

Although ASSLiBs based on inorganic solid electrolytes have clearly demonstrated their great possibilities for electric vehicles and large-scale energy storage systems, further development is still required to improve their energy density, rate capability, and cycling stability, while ensuring excellent safety. Actually, they are still far from being commercialized for industrial applications, which requires systematical studies and will be a complicated process.

Making ASSLiBs usable outside the laboratory involves multiple factors such as solid electrolytes, electrodes, interface properties, and construction design. The high cost and very small production scale of solid state electrolytes with high ionic conductivity hinder the application of ASSLiBs. Meanwhile, ASSLiBs still suffer from inferior power density and poor cycle life, due to the high transfer resistance of lithium ions between the electrodes and solid electrolytes. Thus, at this stage, the direction for research exploring ASSLiBs for commercial applications is to develop new cathodes based on the conversion reaction mechanism with low or even zero strain and energy levels well matched with the electrolytes. All of these together are expected to yield new material systems with high capacity. In addition, the use of lithium metal in anodes will be another thrust of ASSLiB development. Another is the design of novel SEs with high lithium-ion conductivity at room temperature and wide electrochemical window. Meanwhile, future SEs should show excellent chemical stability in the presence of metallic lithium. Also, new methods should be proposed to reduce the interfacial resistance between the electrode and electrolyte. Finally, the optimal combination of different fabrication processes and equipment automation as well

as device design are necessary for the realization of ASSLiBs with high capacity, low cost, and high yield.

In summary, scientific and technical research on ASSLiBs is progressing gradually. The current achievements indicate that ASSLiBs with high energy density are promising candidates for large-scale energy storage and even electric vehicle applications.

References

[1] Xu X, Qiu Z, Guan Y, Huang Z and Jin Y 2013 *Energy Storage Science and Technology* **2** 331 (in Chinese)
[2] Scrosati B and Garche J 2010 *J. Power Sources* **195** 2419
[3] Li W, Dahn J R and Wainwright D S 1994 *Science* **264** 1115
[4] Xu X, Wen Z, Yang X, Zhang J and Gu Z 2006 *Solid State Ionics* **177** 2611
[5] Xu X, Wen Z, Wu J and Yang X 2007 *Solid State Ionics* **178** 29
[6] Kato Y, Kawamoto K, Kanno R and Hirayama M 2012 *Electrochemistry* **80** 749
[7] Takada K 2013 *Acta Mater.* **61** 759
[8] Baba M, Kumagai N, Fujita N, Ohta K, Nishidate K, Komaba S, Groult H, Devilliers D and Kaplan B 2001 *J. Power Sources* **97-8** 798
[9] Gwon H, Hong J, Kim H, Seo D H, Jeon S and Kang K 2014 *Energy Environ. Sci.* **7** 538
[10] Zhang S S, Ervin M H, Xu K and Jow T R 2004 *Electrochim. Acta* **49** 3339
[11] Qiu W, Yang Q, Ma X, Fu Y and Zong X 2004 *Chinese Journal of Power Sources* **28** 440
[12] Ohta N, Takada K, Zhang L, Ma R, Osada M and Sasaki T 2006 *Adv. Mater.* **18** 2226
[13] Bhalla A S, Guo R Y and Roy R 2000 *Mater. Res. Innov.* **4** 3
[14] Inaguma Y, Chen L Q, Itoh M, Nakamura T, Uchida T, Ikuta H and Wakihara M 1993 *Solid State Commun.* **86** 689
[15] Hagman L O and Kierkegaard P 1968 *Acta Chem. Scand* **22** 1822
[16] Goodenough J B, Hong H Y P and Kafalas J A 1976 *Mater. Res. Bull.* **11** 203
[17] Thangadurai V and Weppner W 2006 *Ionics* **12** 81
[18] Subramanian M, Subramanian R and Clearfield A 1986 *Solid State Ionics* **18** 562
[19] Casciola M, Costantino U, Merlini L, Andersen I K and Andersen E K 1988 *Solid State Ionics* **26** 229
[20] Martinezjuarez A, Rojo J M, Iglesias J E and Sanz J 1995 *Chem. Mater.* **7** 1857
[21] Aono H, Sugimoto E, Sadaoka Y, Imanaka N and Adachi G 1990 *Solid State Ionics* **40-1** 38
[22] Morimoto H, Awano H, Terashima J, Shindo Y, Nakanishi S, Ito N, Ishikawa K and Tobishima S I 2013 *J. Power Sources* **240** 636
[23] Xu X, Wen Z, Yang X and Chen L 2008 *Mater. Res. Bull.* **43** 2334
[24] Huang Z, Yang J, Chen X, Tao Y, Liu D, Gao C, Long P and Xu X 2015 *Energy Storage Science and Technology* **4** 1
[25] Xu X, Wen Z, Wu X, Yang X and Gu Z 2007 *J. Am. Ceram. Soc.* **90** 2802
[26] Fu J 1997 *Solid State Ionics* **104** 191
[27] Cruz A M, Ferreira E B and Rodrigues A C M 2009 *J. Non-cryst. Solids.* **355** 2295
[28] Thokchom J S, Gupta N and Kumar B 2008 *J. Electrochem. Soc.* **155** A915
[29] Kasper H M 1969 *Inorg. Chem.* **8** 1000
[30] Mazza D 1988 *Mater. Lett.* **7** 205
[31] Cussen E J 2006 *Chem. Commun.* 412
[32] Thangadurai V, Kaack H and Weppner W J F 2003 *J. Am. Ceram. Soc.* **86** 437
[33] Thangadurai V and Weppner W 2005 *J. Am. Ceram. Soc.* **88** 411
[34] Thangadurai V and Weppner W 2005 *Adv. Funct. Mater.* **15** 107
[35] Thangadurai V and Weppner W 2006 *J. Solid State Chem.* **179** 974
[36] Murugan R, Thangadurai V and Weppner W 2007 *Angew. Chem. Int. Ed.* **46** 7778
[37] Awaka J, Kijima N, Hayakawa H and Akimoto J 2009 *J. Solid State Chem.* **182** 2046
[38] Geiger C A, Alekseev E, Lazic B, Fisch M, Armbruster T, Langner R, Fechtelkord M, Kim N, Pettke T and Weppner W 2011 *Inorg. Chem.* **50** 1089
[39] Murugan R, Ramakumar S and Janani N 2011 *Electrochem. Commun.* **13** 1373
[40] Ohta S, Kobayashi T and Asaoka T 2011 *J. Power Sources* **196** 3342
[41] Allen J L, Wolfenstine J, Rangasamy E and Sakamoto J 2012 *J. Power Sources* **206** 315
[42] Li Y, Han J T, Wang C A, Xie H and Goodenough J B 2012 *J. Mater. Chem.* **22** 15357
[43] Deviannapoorani C, Dhivya L, Ramakumar S and Murugan R 2013 *J. Power Sources* **240** 18
[44] Kennedy J H and Yang Y 1986 *J. Electrochem. Soc.* **133** 2437
[45] Kennedy J H, Sahami S, Shea S W and Zhang Z M 1986 *Solid State Ionics* **18-9** 368
[46] Deshpande V K, Pradel A and Ribes M 1988 *Solid State Ionics* **28** 756
[47] Ahn B T and Huggins R A 1991 *Solid State Ionics* **46** 237
[48] Kondo S, Takada K and Yamamura Y 1992 *Solid State Ionics* **53** 1183
[49] Mizuno F, Hayashi A, Tadanaga K, Minami T and Tatsumisago M 2004 *Solid State Ionics* **175** 699
[50] Morimoto H, Yamashita H, Tatsumisago M and Minami T 1999 *J. Am. Ceram. Soc.* **82** 1352
[51] Kanno R and Maruyama M 2001 *J. Electrochem. Soc.* **148** A742
[52] Mizuno F, Hayashi A, Tadanaga K and Tatsumisago M 2005 *Adv. Mater.* **17** 918
[53] Mizuno F, Hayashi A, Tadanaga K and Tatsumisago M 2006 *Solid State Ionics* **177** 2721
[54] Hayashi A, Hama S, Minami T and Tatsumisago M 2003 *Electrochem. Commun.* **5** 111
[55] Tatsumisago M, Hama S, Hayashi A, Morimoto H and Minami T 2002 *Solid State Ionics* **154** 635
[56] Tachez M, Malugani J P, Mercier R and Robert G 1984 *Solid State Ionics* **14** 181
[57] Liu Z, Fu W, Payzant E A, Yu X, Wu Z, Dudney N J, Kiggans J, Hong K, Rondinone A J and Liang C 2013 *J. Am. Chem. Soc.* **135** 975
[58] Rangasamy E, Liu Z, Gobet M, Pilar K, Sahu G, Zhou W, Wu H, Greenbaum S and Liang C 2015 *J. Am. Chem. Soc.* **137** 1384
[59] Shin B R, Nam Y J, Oh D Y, Kim D H, Kim J W and Jung Y S 2014 *Electrochim. Acta* **146** 395
[60] Muramatsu H, Hayashi A, Ohtomo T, Hama S and Tatsumisago M 2011 *Solid State Ionics* **182** 116
[61] Hayashi A, Muramatsu H, Ohtomo T, Hama S and Tatsumisago M 2014 *J. Alloy. Compd.* **591** 247
[62] Xu X, Takada K, Fukuda K, Ohnishi T, Akatsuka K, Osada M, Bui Thi H, Kumagai K, Sekiguchi T and Sasaki T 2011 *Energy Environ. Sci.* **4** 3509
[63] Xu X, Takada K, Watanabe K, Sakaguchi I, Akatsuka K, Hang B T, Ohnishi T and Sasaki T 2011 *Chem. Mater.* **23** 3798
[64] Minami K, Hayashi A, Ujiie S and Tatsumisago M 2011 *Solid State Ionics* **192** 122
[65] Seino Y, Ota T, Takada K, Hayashi A and Tatsumisago M 2014 *Energy Environ. Sci.* **7** 627
[66] Kamaya N, Homma K, Yamakawa Y, Hirayama M, Kanno R, Yonemura M, Kamiyama T, Kato Y, Hama S, Kawamoto K and Mitsui A 2011 *Nat. Mater.* **10** 682
[67] Kuhn A, Duppel V and Lotsch B V 2013 *Energy Environ. Sci.* **6** 3548
[68] Bron P, Johansson S, Zick K, auf der Guenne J S, Dehnen S and Roling B 2013 *J. Am. Chem. Soc.* **135** 15694
[69] Tatsumisago M, Nagao M and Hayashi A 2013 *Journal of Asian Ceramic Societies* **1** 17
[70] Sakuda A, Hayashi A, Ohtomo T, Hama S and Tatsumisago M 2010 *Electrochemical and Solid-State Letters* **13** A73
[71] Kitaura H, Hayashi A, Tadanaga K and Tatsumisago M 2010 *Electrochim. Acta* **55** 8821
[72] Seino Y, Ota T and Takada K 2011 *J. Power Sources* **196** 6488
[73] Iwasaki S, Hamanaka T, Yamakawa T, West W C, Yamamoto K, Motoyama M, Hirayama T and Iriyama Y 2014 *J. Power Sources* **272** 1086
[74] Kitaura H, Hayashi A, Tadanaga K and Tatsumisago M 2010 *J. Electrochem. Soc.* **157** A407

[75] Yada C, Ohmori A, Ide K, Yamasaki H, Kato T, Saito T, Sagane F and Iriyama Y 2014 *Adv. Energy Mater.* **4** 1301416

[76] Nagao M, Hayashi A, Tatsumisago M, Ichinose T, Ozaki T, Togawa Y and Mori S 2015 *J. Power Sources* **274** 471

[77] Nagao M, Hayashi A and Tatsumisago M 2012 *J. Mater. Chem.* **22** 10015

[78] Nagao M, Hayashi A and Tatsumisago M 2011 *Electrochim. Acta* **56** 6055

[79] Hayashi A, Ohtsubo R and Tatsumisago M 2008 *Solid State Ionics* **179** 1702

[80] Shin B R, Nam Y J, Kim J W, Lee Y G and Jung Y S 2014 *Scientific Reports* **4** 5572

[81] Yersak T A, Stoldt C and Lee S H 2013 *J. Electrochem. Soc.* **160** A1009

[82] Yersak T A, Evans T, Whiteley J M, Son S B, Francisco B, Oh K H and Lee S H 2014 *J. Electrochem. Soc.* **161** A663

[83] Aso K, Kitaura H, Hayashi A and Tatsumisago M 2011 *J. Mater. Chem.* **21** 2987

[84] Aso K, Sakuda A, Hayashi A and Tatsumisago M 2013 *Acs Appl. Mater. Interfaces* **5** 686

[85] Haruyama J, Sodeyama K, Han L, Takada K and Tateyama Y 2014 *Chem. Mater.* **26** 4248

[86] Sakuda A, Hayashi A and Tatsumisago M 2010 *Chem. Mater.* **22** 949

[87] Sakuda A, Nakamoto N, Kitaura H, Hayashi A, Tadanaga K and Tatsumisago M 2012 *J. Mater. Chem.* **22** 15247

[88] Sakuda A, Hayashi A, Ohtomo T, Hama S and Tatsumisago M 2011 *J. Power Sources* **196** 6735

[89] Ohta N, Takada K, Sakaguchi I, Zhang L, Ma R, Fukuda K, Osada M and Sasaki T 2007 *Electrochem. Commun.* **9** 1486

[90] Sakuda A, Kitaura H, Hayashi A, Tadanaga K and Tatsumisago M 2009 *J. Power Sources* **189** 527

[91] Woo J H, Trevey J E, Cavanagh A S, Choi Y S, Kim S C, George S M, Oh K H and Lee S H 2012 *J. Electrochem. Soc.* **159** A1120

[92] Teragawa S, Aso K, Tadanaga K, Hayashi A and Tatsumisago M 2014 *J. Power Sources* **248** 939

[93] Teragawa S, Aso K, Tadanaga K, Hayashi A and Tatsumisago M 2014 *J. Mater. Chem. A* **2** 5095

[94] Ohzuku T and Makimura Y 2001 *Chem. Lett.* 642

[95] Meng H, Huang B, Yin J, Yao X and Xu X 2015 *Ionics* **21** 43

[96] Machida N, Kashiwagi J, Naito M and Shigematsu T 2012 *Solid State Ionics* **225** 354

[97] Okada K, Machida N, Naito M, Shigematsu T, Ito S, Fujiki S, Nakano M and Aihara Y 2014 *Solid State Ionics* **255** 120

[98] Tan G, Wu F, Lu J, Chen R, Li L and Amine K 2014 *Nanoscale* **6** 10611

[99] Heidy V, Satoshi F, Aihara Y, Taku W, Youngsin P and Doo S 2014 *J. Power Sources* **269** 396

[100] Uemura T, Goto K, Ogawa M and Harada K 2013 *J. Power Sources* **240** 510

[101] Ito S, Fujiki S, Yamada T, Aihara Y, Park Y, Kim T Y, Baek S W, Lee J M, Doo S and Machida N 2014 *J. Power Sources* **248** 943

[102] Kitaura H, Hayashi A, Tadanaga K and Tatsumisago M 2011 *Solid State Ionics* **192** 304

[103] Lin Z and Liang C 2015 *J. Mater. Chem. A* **3** 936

[104] Barghamadi M, Best A S, Bhatt A I, Hollenkamp A F, Musameh M, Rees R J and Rüther T 2014 *Energy Environ. Sci.* **7** 3902

[105] Jung Y S, Oh D Y, Nam Y J and Park K H 2015 *Israel J. Chem.*

[106] Hayashi A, Ohtsubo R, Ohtomo T, Mizuno F and Tatsumisago M 2008 *J. Power Sources* **183** 422

[107] Nagata H and Chikusa Y 2014 *J. Power Sources* **264** 206

[108] Takeuchi T, Kageyama H, Nakanishi K, Tabuchi M, Sakaebe H, Ohta T, Senoh H, Sakai T and Tatsumi K 2010 *J. Electrochem. Soc.* **157** A1196

[109] Lin Z, Liu Z, Dudney N J and Liang C 2013 *ACS Nano* **7** 2829

[110] Nagao M, Kitaura H, Hayashi A and Tatsumisago M 2013 *J. Electrochem. Soc.* **160** A819

[111] Nagao M, Hayashi A, Tatsumisago M, Kanetsuku T, Tsuda T and Kuwabata S 2013 *Phys. Chem. Chem. Phys.* **15** 18600

[112] Sahu G, Lin Z, Li J, Liu Z, Dudney N and Liang C 2014 *Energy Environ. Sci.* **7** 1053

[113] Takahara H, Tabuchi M, Takeuchi T, Kageyama H, Ide J, Handa K, Kobayashi Y, Kurisu Y, Kondo S and Kanno R 2004 *J. Electrochem. Soc.* **151** A1309

[114] Takada K, Aotani N, Iwamoto K and Kondo S 1996 *Solid State Ionics* **86-8** 877

[115] Jung Y S, Lee K T, Kim J H, Kwon J Y and Oh S M 2008 *Adv. Funct. Mater.* **18** 3010

[116] Seino Y, Takada K, Kim B C, Zhang L Q, Ohta N, Wada H, Osada M and Sasaki T 2005 *Solid State Ionics* **176** 2389

[117] Takeuchi T, Kageyama H, Nakanishi K, Ohta T, Sakuda A, Sakai T, Kobayashi H, Sakaebe H, Tatsumi K and Ogumi Z 2014 *Solid State Ionics* **262** 138

[118] Takada K, Inada T, Kajiyama A, Sasaki H, Kondo S, Watanabe M, Murayama M and Kanno R 2003 *Solid State Ionics* **158** 269

[119] Takada K, Nakano S, Inada T, Kajiyama A, Sasaki H, Kondo S and Watanabe M 2003 *J. Electrochem. Soc.* **150** A274

[120] Haik O, Leifer N, Samuk-Fromovich Z, Zinigrad E, Markovsky B, Larush L, Goffer Y, Goobes G and Aurbach D 2010 *J. Electrochem. Soc.* **157** A1099

[121] Trevey J E, Jung Y S and Lee S H 2011 *Electrochim. Acta* **56** 4243

[122] Hayashi A and Tatsumisago M 2012 *Electronic Materials Letters* **8** 199

[123] Kim J, Eom M, Noh S and Shin D 2013 *J. Power Sources* **244** 476

[124] Trevey J E, Stoldt C R and Lee S H 2011 *J. Electrochem. Soc.* **158** A1282

[125] Hayashi A, Nishio Y, Kitaura H and Tatsumisago M 2008 *Electrochem. Commun.* **10** 1860

[126] Kitaura H, Hayashi A, Ohtomo T, Hama S and Tatsumisago M 2011 *J. Mater. Chem.* **21** 118

[127] Sakuda A, Kitaura H, Hayashi A, Tadanaga K and Tatsumisago M 2009 *J. Electrochem. Soc.* **156** A27

[128] Sakuda A, Kitaura H, Hayashi A, Tadanaga K and Tatsumisago M 2008 *Electrochem. Solid State Lett.* **11** A1

[129] Kim K H, Iriyama Y, Yamamoto K, Kumazaki S, Asaka T, Tanabe K, Fisher C A J, Hirayama T, Murugan R and Ogumi Z 2011 *J. Power Sources* **196** 764

[130] Okumura T, Nakatsutsumi T, Ina T, Orikasa Y, Arai H, Fukutsuka T, Iriyama Y, Uruga T, Tanida H, Uchimoto Y and Ogumi Z 2011 *J. Mater. Chem.* **21** 10051

[131] Takada K 2013 *Langmuir* **29** 7538

[132] Takada K, Ohta N and Tateyama Y 2015 *Journal of Inorganic and Organometallic Polymers and Materials* **25** 205

[133] Takada K, Ohta N, Zhang L, Xu X, Bui Thi H, Ohnishi T, Osada M and Sasaki T 2012 *Solid State Ionics* **225** 594

[134] Yamada H, Oga Y, Saruwatari I and Moriguchi I 2012 *J. Electrochem. Soc.* **159** A380

[135] Kishida K, Wada N, Yamaguchi Y, Tanaka K, Iriyama Y, Ogumi Z and Inui H 2007 in *Solid-State Ionics-2006* (Traversa E, Armstrong T R, Masquelier C and Sadaoka Y Eds.) 2007 vol. **972** p. 251

[136] http://techon.nikkeibp.co.jp/english/NEWS_EN/20101122/187553/

[137] Tsuchiya H, Aihara Y, Fujiki S, Yamada T, Park Y and Doo S K 2014 225th ECS Meeting, May 11–15, 2014, Orlando USA, p. 107